



Analytical Approach of Fe₃O₄-Ethylene Glycol Radiative Magnetohydrodynamic Nanofluid on Entropy Generation in a Shrinking Wall with Porous Medium

U. Humphries^a, M. Govindaraju^b, P. Kaewmesri^a, P. Hammachukiattikul^c, B. Unyong^c, G. Rajchakit^{*d}, R. Vadivel^e, N. Gunasekaran^e

^a Department of Mathematics, Faculty of Science, King Mongkut's University of Technology Thonburi (KMUTT), ThungKhru, Thailand

^b Department of Mathematics, Padmavani Arts and Science College for Women, Salem, Periyar University, Tamil Nadu, India

^c Department of Mathematics, Faculty of Science and Technology, Phuket Rajabhat University, Phuket, Thailand

^d Department of Mathematics, Faculty of Science, Maejo University, Chiang Mai, Thailand

^e Department of Mathematical Sciences, Shibaura Institute of Technology, Saitama, Japan

PAPER INFO

Paper history:

Received 29 September 2020

Received in revised form 04 November 2020

Accepted 10 November 2020

Keywords:

Entropy

Fe₃O₄-Ethylene Glycol Nanofluid

Heat Absorption

Heat Generation

Shrinking Wall

ABSTRACT

This research mainly focuses on the effects of heat absorption/generation and radiation on the hydromagnetic flow of Fe₃O₄-ethylene glycol nanofluid through a shrinking wall with porous medium and the computation of the entropy generation. We considered basic governing ordinary differential equations into partial differential equations by using appropriate similarity solutions. Moreover, hyper geometric function is employing to determine the formulated problem. We analyze the effects of appropriate physical parameters on the Bejan number, Entropy generation, Nussult number, skin friction, fluid temperature and velocity profiles. In addition, the derived result of the present study is compared with those in the existing literature. We noted that the presence of heat absorption and suction parameters reduces the Bejan number and increases the entropy generation, and the heat source, porous medium, radiation parameters minimize the entropy production. The presence of porosity parameter reduced the fluid velocity, improved fluid temperature and minimized the entropy production. Nanosolid volume fraction parameter reduced both Nussult number and skin friction coefficient.

doi: 10.5829/ije.2021.34.02b.25

NOMENCLATURE

\cdot	magnetic field strength	T_w	wall temperature
Br	Brinkman number	T_∞	temperature far away from the sheet
C_p	specific heat at constant temperature	k_{nf}	thermal conductivity of the nanofluid
M_3	Hartmann number	k_f	thermal conductivity of the base fluid
M	Kummer's function	k_s	thermal conductivity of the nanoparticles
Nr	radiation parameter	k^*	The absorption coefficient of the fluid
Ns	entropy generation number	σ	electric conductivity
Pr	Prandtl number	σ^*	Stephan-Boltzman constant
T	local temperature of the fluid	S_{G0}	characteristic entropy generation rate
Q	Temperature dependent volumetric rate of heat source	ΔT	temperature difference
Qr	radiative heat flux	Ω	dimensionless temperature difference
Re_x	Reynolds number	θ	dimensionless temperature
S	Suction parameter	ϕ	the solid volume fraction
S_G	local volumetric Entropy generation rate	β	uniform heat generation/absorption

*Corresponding Author Institutional Email: kreangkri@mju.ac.th (G. Rajchakit)

Please cite this article as: U. Humphries, M. Govindaraju, P. Kaewmesri, P. Hammachukiattikul, B. Unyong, G. Rajchakit, R. Vadivel, N. Gunasekaran, Analytical Approach of Fe₃O₄-Ethylene Glycol Radiative Magnetohydrodynamic Nanofluid on Entropy Generation in a Shrinking Wall with Porous Medium, International Journal of Engineering, B: Applications Vol. 34, No. 02, (2021) 517-527

1. INTRODUCTION

There are several systematic challenges pertaining to efficient heat transfer of heat in different processes, example, in batteries, drug formulation, chemical reactions, fuel cells, solar cells, and others. This phenomenon has been studied through the field of nanotechnology. The most important performance of nanotechnology is nanofluids. Many scientific and technological fields utilize nanofluid models. Choi [1] introduced the notion of increase in the thermal conductivity of nanofluid. Ibrahim et al. [2] analyzed the nanofluid heat transfer effects with hydromagnetic and stagnation point flow numerically. Various types of nanoparticle, including Cu, Ag, Al_2O_3 and TiO_2 , used in the base fluid towards a porous stretching surface has been examined by Hayat et al. [3]. Al_2O_3 -water with hydromagnetic flow towards a vertical microtube for enhancement of the heat transfer rate has been researched by Malvandi and Ganji [4]. The effects of flow towards a shrinking sheet using nanofluid with slip conditions have been developed by Rahman et al. [5]. The phenomenon of flow through a shrinking porous sheet, along with analytical result of Fe_3O_4 -water hydrodynamic nanofluid flow was researched by shaha et al. [6].

Over the most recent few decades, incredible interest has been shown by scientists on the subject of stretching surfaces with magnetic field because of its colossal applications in various mechanical and engineering procedures. Some of these fascinating and amazing applications are glass plastic expulsion, fiber drawing, crystal developing, petroleum industries, paper creation, plasma studies, etc. Heat transfer effects in CuO-water nanofluid flow with magnetic field were analyzed by Sheikholeslami et al. [7]. Jamaludin et al. [8] researched the effects of shrinking surface flow of heat generation or absorption and hydromagnetic Cu and Al_2O_3 based hybrid nanofluid flow numerically. Heat conduction effects on shrinking porous surface with Cu and Ag - $\text{C}_6\text{H}_9\text{NaO}_7$ Corrosion based nanofluids flow has been studied by Dero et al. [9]. It is clear that copper and silver based volume fraction nanoparticle improves the thermal conduction and reduces the fluid velocity. Heat conduction effects of shrinking porous surface with thermal radiation and copper based nanofluid flow were studied by Haq et al. [10]. Heat conduction of various types of nanofluid flow towards shrinking surface was reported in literature [11-14].

On the other hand, entropy represents an irreversibility process and it is utilized to enhance the capacity of machine. The entropy models can be related to manufacturing and engineering processes pertaining to nanofluids. This has been an active research area recently. Hayat et al. [15] investigated thermal irreversibility analysis for energy activation and non-linear thermal radiation of Jeffrey nanofluid flow towards

stretchable sheet. Hosseinzadeh et al. [16] studied thermal irreversibility analysis for Fe_3O_4 -Ethylene glycol nanofluid with nonlinear thermal radiation and Lorentz force effects. Shahsavari et al. [17] presented an analysis of heat and irreversibility study of Fe_3O_4 nanofluid flow through a concentric annulus. Mehrali et al. [18] researched the impacts of Fe_3O_4 nanofluid flow and conducted an analysis of entropy on magnetic. Very recently, López et al. [19] investigated the effects of Al_2O_3 nanofluid flow and analyzed the entropy on hydromagnetic, nonlinear radiation and slip conditions. Shukla et al. [20] have studied a homotopy method for irreversibility analysis of vertical cylinder flow of viscous dissipation and magnetohydrodynamic (MHD) nanofluid flow. Hayat et al. [21], investigated on MHD nonlinear thermal radiation and joule heating effects with respect to nanofluid flow with entropy analysis has been conducted. Rana and Shukla [22] provided an analytical solution for an irreversibility study of aligned MHD nanofluid flow towards a plate with Ohmic dissipation and viscous dissipation effects.

The study of boundary layer MHD nanofluid flow and heat transfer due shrinking wall with porous medium is very significant because of its several applications in engineering and industrial processes, such as extrusion of polymer sheets from a die, drawing of plastic films, polyester thin wall heat shrink tubing, shrink film, wire drawing, glass fiber, and paper production. Govindaraju et al. [23] researched the irreversibility mechanism of Ag-water MHD nanofluid fluid flow with heat source or sink and radiation effects. Abdul Hakeem et al. [24] presented the non-uniform heat source or sink and radiation effects on Ag-water MHD nanofluid flow, along with the analysis of entropy. Ganga et al. [25] researched the effects of the irreversibility and Ag-water inclined MHD nanofluid flow towards a stretching sheet. Recently, the irreversibility phenomenon of various types of nanofluid flow was investigated by many researchers [26-32]. Some researchers reported data by demonstration of experimental work [33-38]. To the best of author's knowledge, upto now, no theoretical results are given for the effects of heat transfer and irreversibility of hydromagnetic Fe_3O_4 -ethylene glycol nanofluid flow in a shrinking wall with porous medium, heat sink or source and thermal radiation. This is the main motivation of our present study.

Motivated by the above discussions, we designed analytically the heat sink or source, MHD and thermal radiation effects on Fe_3O_4 -ethylene glycol nanofluid flow in a shrinking wall with porous medium. The fluid velocity, heat transfer process, Bejan number and the irreversibility phenomenon, skin friction co-efficient and temperature transfer rate are examined with the graphs, in which our solutions are in good agreement with earlier published results.

The contents of this paper are divided up as follows:

The description of physical model is clearly prescribed in section 2. In this section, the mathematical model for the 2-Dimensional incompressible flow of Fe₃O₄-ethylene glycol based nanofluid has been presented. Section 3 is devoted to the solution of these models equations by hyper geometric function method. The Entropy generation and Bejan number has been computed in section 4. The results and discussion has been presented in section 5. Finally, the main findings of the current study have been given in section 6.

2. MATHEMATICAL ANALYSIS

In this investigation, consider the incompressible 2-dimensional flow of Fe₃O₄-Ethylene glycol based nanofluid towards a shrinking wall with porous medium. The fluid flow is along the x-axis (horizontal) and the y-axis is the vertical dimension, then $y > 0$ is the occupied volume of the fluid. Suppose normal to the flow of an applied magnetic field is $B(x)$ with velocity $u = ax$ (Figure 1). The two-dimensional thermal radiation with magnetohydrodynamic flow of governing equations are given, as follows [26, 39-41] (Figure 2):

$$\frac{\partial u}{\partial x} + \frac{\partial v}{\partial y} = 0 \tag{1}$$

$$u \frac{\partial u}{\partial x} + v \frac{\partial u}{\partial y} = \frac{\mu_{nf}}{\rho_{nf}} \frac{\partial^2 u}{\partial y^2} - \frac{v_{nf}}{K_p} u - \frac{\sigma_{nf} B(x)^2}{\rho_{nf}} u \tag{2}$$

$$u \frac{\partial T}{\partial x} + v \frac{\partial T}{\partial y} = \alpha_{nf} \frac{\partial^2 T}{\partial y^2} - \frac{1}{(\rho C_p)_{nf}} \frac{\partial q_r}{\partial y} + \frac{Q(T-T_\infty)}{(\rho C_p)_{nf}} \tag{3}$$

Here u and v denote the velocity components along the x -axis and the y -axis, respectively; $B(x)$ represents the magnetic parameter; ν_{nf} , μ_{nf} , ρ_{nf} , α_{nf} denote the kinematic viscosity, dynamic viscosity, density, thermal diffusivity, respectively. The subscript nf indicates the nanofluid; T denoted as fluid temperature, while Q represents the volumetric heat sink or source rate. The heat flux q_r , [26, 41] through the Rosseland approximation is defined as:

$$q_r = -\frac{\sigma^*}{3k^*} \frac{\partial T^4}{\partial y} \tag{4}$$

Here k^* is the absorption coefficient of the fluid, from Equations (3) and (4), we have

$$u \frac{\partial T}{\partial x} + v \frac{\partial T}{\partial y} = \alpha_{nf} \frac{\partial^2 T}{\partial y^2} - \frac{16\sigma^* T_\infty^3}{3k^*(\rho C_p)_{nf}} \frac{\partial^2 T}{\partial y^2} + \frac{Q(T-T_\infty)}{(\rho C_p)_{nf}} \tag{5}$$

The heat conductivity can be expressed as follows:

$$\begin{aligned} \mu_{nf} &= \frac{\mu_f}{(1-\phi)^{2.5}}, & \rho_{nf} &= (1-\phi)\rho_f + \phi\rho_s \\ (\rho C_p)_{nf} &= (1-\phi)(\rho C_p)_f + \phi(\rho C_p)_s, \\ k_{nf} &= \frac{k_s + 2k_f - 2\phi(k_f - k_s)}{k_s + 2k_f - \phi(k_f - k_s)}, & \alpha_{nf} &= \frac{k_{nf}}{(\rho C_p)_{nf}} \end{aligned} \tag{6}$$

$$\frac{\sigma_{nf}}{\sigma_f} = 1 + \frac{3\left(\frac{\sigma_{nf}}{\sigma_f} - 1\right)\phi}{\left(\frac{\sigma_{nf}}{\sigma_f} + 2\right) - \left(\frac{\sigma_{nf}}{\sigma_f} - 1\right)\phi}$$

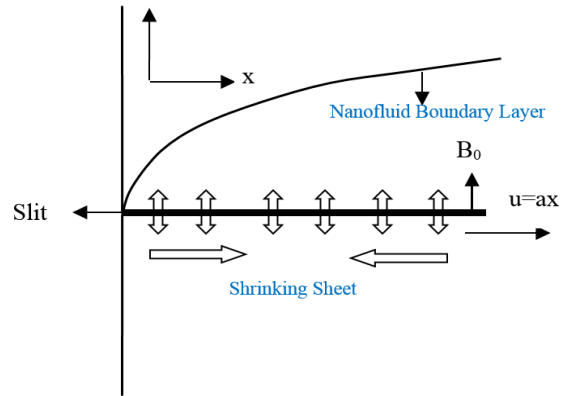


Figure 1. Schematic representation of the flow diagram

where the physical problem of the surface conditions is

$$\begin{aligned} u &= -U_x, v = -v_x, T = T_w = T_\infty + T_0(x)^n, \text{ at } y = 0, \\ u \rightarrow u = 0, & \quad T \rightarrow T_\infty, \text{ as } y \rightarrow \infty. \end{aligned} \tag{7}$$

Here, v_x noted as wall mass transfer velocity; in which $v_x < 0$ and $v_x > 0$ are the injection and suction parameters. The non-dimensional and similarity variables are [26, 42, 43].

$$\begin{aligned} u &= axf'(\eta), v = -(va)^{\frac{1}{2}} f(\eta), \theta(\eta) = \frac{T - T_\infty}{T_w - T_\infty} \\ \eta &= y \left(\frac{a}{\nu}\right)^{\frac{1}{2}} \end{aligned} \tag{8}$$

After applying the similarity transformation of Equations (2) and (3), we have

$$f''' + B_1 B_2 f f'' - B_1 B_2 f'^2 - B_2 (M_3 - B_1 k) f' = 0 \tag{9}$$

$$\omega \theta'' + Pr f \theta' - n Pr f' \theta + \beta Pr \theta = 0. \tag{10}$$

With

$$f(\eta) = S, f'(\eta) = -1, \theta(\eta) = 1 \text{ at } \eta = 0 \quad f'(0) \rightarrow 0, \theta(\eta) \rightarrow 0 \text{ as } \eta \rightarrow \infty \tag{11}$$

Based on Equations (9), (10) and (11), Prandtl number $Pr = \frac{\nu_f}{\alpha_f}$, porosity parameter $k = \frac{\nu_f}{aK_p}$, $\beta = \frac{Q}{a(\rho C_p)_f}$ noted heat sink or source parameter, $M_3 = \frac{2L\sigma B_0^2}{\rho}$ noted as Hartmann number. In addition,

$$\begin{aligned} B_1 &= \left(1 - \phi \left(1 - \frac{\rho_s}{\rho_f}\right)\right), & B_2 &= (1 - \phi)^{5/2}, & B_3 &= \frac{k_{nf}}{k_f}, \\ B_4 &= 1 - \phi + \phi \frac{(\rho C_p)_s}{(\rho C_p)_f}, & \omega &= \frac{B_3}{B_4} \frac{3NrB_3 + 4}{3NrB_3}, & Nr &= \frac{k^* k_f}{4\sigma^* T_\infty^3}. \end{aligned}$$

3. ANALYTICAL SOLUTION OF FLOW FIELD AND THERMAL ANALYSIS

The shrinking sheet fluid flow solution of (9) with (11) is obtained as follows [26, 41]:

$$f(\eta) = S - \frac{1 - e^{-\alpha\eta}}{\alpha}, \tag{12}$$

with $\alpha = \frac{SB_1B_2 + \sqrt{(SB_1B_2)^2 - 4B_1B_2 + 4B_2M_3 - 4kB_1B_2}}{2}$

Substituting Equation (12) into Equation (10), we have

$$\omega\theta'' + Pr\left(S - \left(\frac{1 - e^{-\alpha\eta}}{\alpha}\right)\right)\theta' - nPre^{-\alpha\eta}\theta + \beta Pr\theta = 0. \tag{13}$$

Here, we introduce a new variable

$$\xi = \frac{Pre^{-\alpha\eta}}{\omega\alpha^2} \tag{14}$$

Substituting Equation (14) into Equation (13), we have

$$\xi\theta_{\xi\xi} + (1 - a_0 + \xi)\theta_{\xi} + \left(n + \frac{\beta Pr}{\omega\alpha^2\xi}\right)\theta = 0. \tag{15}$$

From Equation (11), it becomes

$$\theta(\xi) = 1, \theta(0) = 0. \tag{16}$$

Using Kummer's function [26,43], we obtain the solution of Equations (14), (15), and (16), in terms of η

$$\theta(\eta) = e^{-\alpha\left(\frac{a_0+b_0}{2}\right)\eta} \frac{M\left[\frac{a_0+b_0}{2} - n; 1 + b_0; \frac{Pre^{-\alpha\eta}}{\omega\alpha^2}\right]}{M\left[\frac{a_0+b_0}{2} - n; 1 + b_0; \frac{Pr}{\omega\alpha^2}\right]} \tag{17}$$

where $a_0 = \frac{Pr}{\omega\alpha}\left(S - \frac{1}{\alpha}\right)$, $b_0 = \sqrt{a_0^2 - 4\frac{\beta Pr}{\omega\alpha^2}}$.

The dimensionless wall temperature gradient is

$$\theta'(0) = -\alpha\left(\frac{a_0+b_0}{2}\right) + \frac{\frac{a_0+b_0}{2} - n}{1 + b_0} \frac{M\left[\frac{a_0+b_0}{2} + 2 - n; 2 + b_0; \frac{Pr}{\omega\alpha^2}\right]}{M\left[\frac{a_0+b_0}{2} - n; 1 + b_0; \frac{Pr}{\omega\alpha^2}\right]}. \tag{18}$$

We denote the skin friction and Nusselt number as

$$C_f = \frac{\tau_w}{\rho u_w^2} = \frac{Re_x^{-1/2}}{B_1} f''(0), B_1 C_f Re_x^{-1/2} = -f''(0)$$

$$Nu = \frac{-k_{nf}x\left(\frac{\partial T}{\partial y}\right)_{y=0}}{k_f(T_w - T_\infty)} = -\frac{k_{nf}}{k_f} Re_x^{-1/2} \theta'(0), \tag{19}$$

$$\frac{k_f}{k_{nf}} Nu_x Re_x^{-1/2} = -\theta'(0)$$

4. ANALYSIS OF ENTROPY AND BEJAN NUMBER

Now, using the second law of thermodynamics, the analysis of entropy generation expression of magnetohydrodynamic nanofluid flow with thermal radiation is given by

$$S_G = \frac{k_{nf}}{T_\infty^2} \left[\left(\frac{\partial T}{\partial x}\right)^2 + \left(1 + \frac{16\sigma^* T_\infty^3}{3k_{nf}k_{nf}}\right) \left(\frac{\partial T}{\partial y}\right)^2 \right] + \frac{\mu_{nf}}{T_\infty} \left(\frac{\partial u}{\partial y}\right)^2 + \frac{\sigma B_0^2}{T_\infty} u^2 + \frac{\nu_{nf}}{k_{nf}} u^2 \tag{20}$$

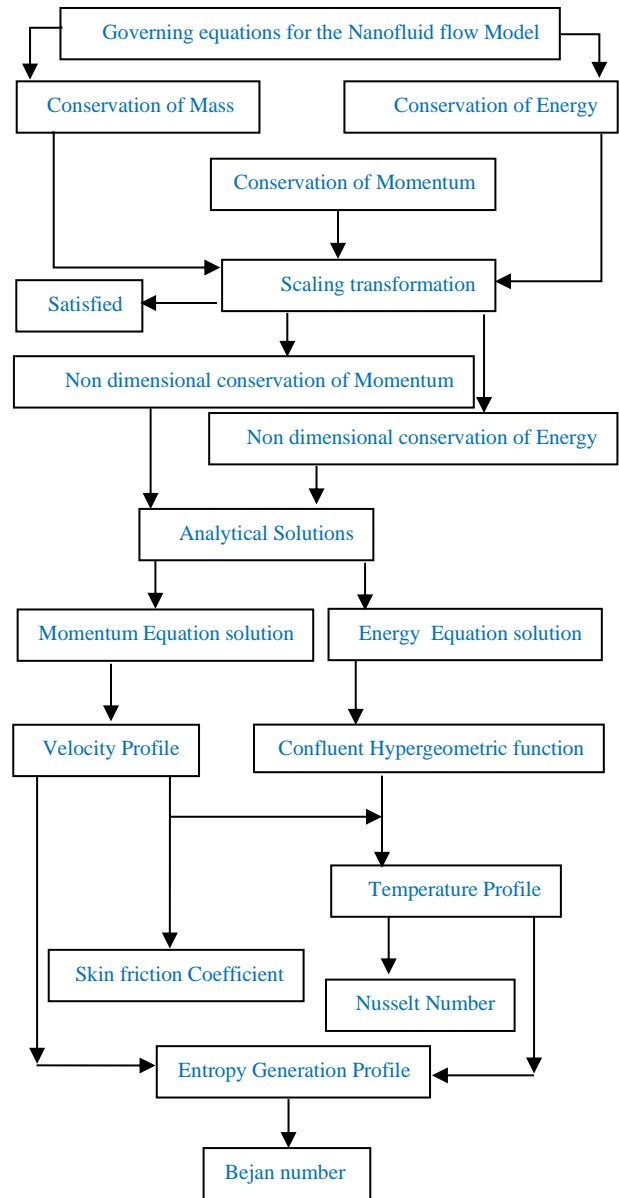


Figure 2. Flowchart of the study

The rate of entropy generation characteristic is given by

$$(S_G)_0 = \frac{k_{nf}(\Delta T)^2}{x^2 T_\infty^2}. \tag{21}$$

Using Equations (20) and (21), we obtain the entropy generation number

$$N_s = \frac{S_G}{(S_G)_0}. \tag{22}$$

From Equations (17), (20), (21) and (22), we can specify the entropy generation number as

$$N_s = \left(\frac{3+4Nr}{3}\right)\theta'^2(\eta)Re_x + \frac{Br}{\Omega} f''^2(\eta)Re_x + \frac{Br}{\Omega} (M_3 + k) f'^2(\eta), \tag{23}$$

where Br is the Brinkman number and Hartmann number denoted as M_3 .

$$Br = \frac{\mu_n f u_w^2}{k_n f \Delta T}, \quad \Omega = \frac{\Delta T}{T_\infty} \tag{24}$$

The Bejan number (Be) was proposed by Bejan with respect to the energy optimization problem utilized by the solution of thermal irreversibility. Thermal irreversibility pertaining to the sum of all entropy in the model is given as:

$$Be = \frac{Eh}{Eh + Em} \tag{25}$$

5. RESULTS AND DISCUSSION

In this study, the analytical solutions are established for Fe_3O_4 -ethylene glycol nanofluid through a shrinking wall with porous medium and the computation of entropy generation is analyzed. Figures 3 to 21 depict the effects of various important physical parameters, including the Bejan number, velocity of the fluid, Nusselt number, heat profile, entropy generation and skin friction co-efficient. The important physical parameters, nanosolid volume fraction (ϕ), heat sink or source (β), porosity parameter (k), radiation parameter (Nr), Hartmann number (M_3), suction parameter (S) effects are analyzed based on the trends in the respective figures. The current results have been discussed to the solutions achieved by Muhaimin et al. [39] and Bhattacharyya [40] (see Table 2). The presented results showed a good agreement with data reported in literature [39, 40].

5. 1. Fluid Flow and Heat Transfer

The profiles of fluid velocity along with various settings of the

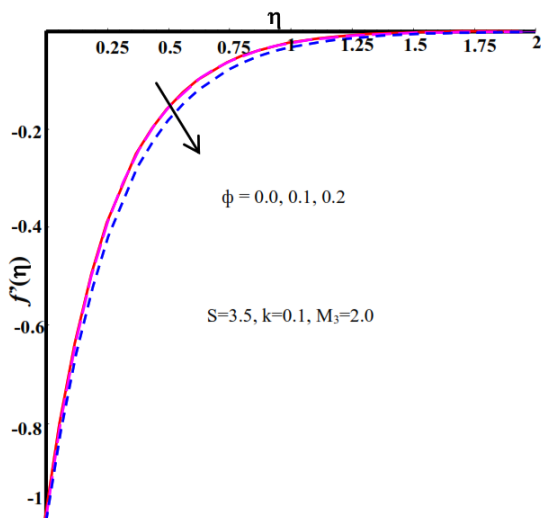


Figure 3. Impact of nanoparticles volume fraction parameter on $f'(\eta)$

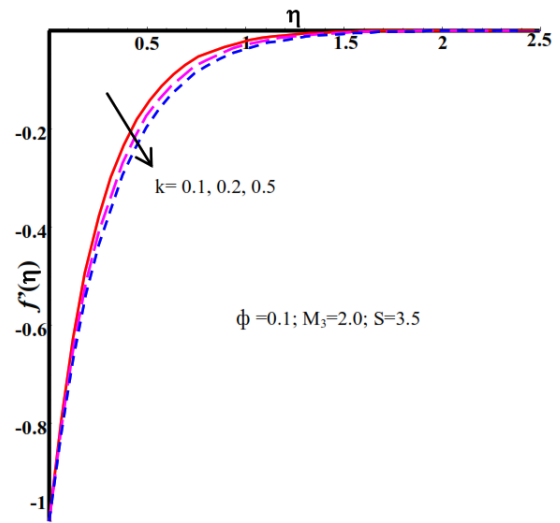


Figure 4. Impact of porosity parameter on $f'(\eta)$

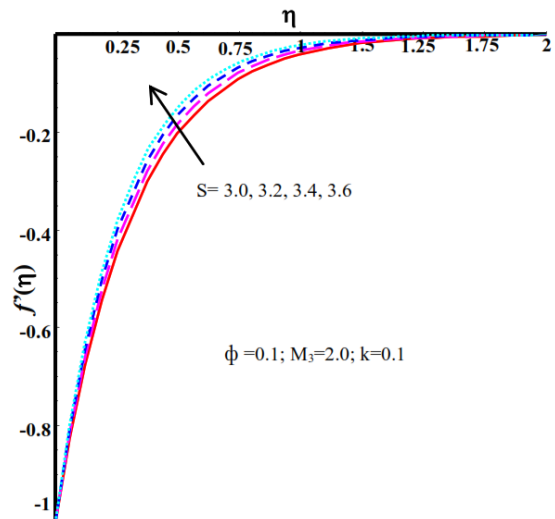


Figure 5. Impact of suction parameter on $f'(\eta)$

nanosolid volume fraction, suction and porosity parameters are presented in Figures 3-5, respectively. From these figures, increasing the porosity and nanosolid volume fraction parameters result in a reduction of the fluid flow, while increasing the suction parameters causes enhancing the fluid flow. The presence of both porosity and nanosolid volume fraction slows down the fluid velocity. The impact of ϕ variation on $f'(\eta)$ is presented in Figure 3, while the variation of porosity parameter on $f'(\eta)$ is represented in Figure 4. Figure 5 demonstrates the evolution of suction parameter on $f'(\eta)$. It is noted that the enhancing of ϕ and k reduces $f'(\eta)$, while increasing S leads to a reduction in $f'(\eta)$.

The thermal profile for various settings of the nanosolid volume fraction, porosity, suction, radiation, heat sink or source parameters are presented in Figures 6-10, respectively. Increasing the value of Fe_3O_4

nanoparticle leads to a development of heat conduction in Ethylene glycol based nanofluid. The porosity parameter also increases heat conduction in Ethylene glycol based nanofluid. But, the presence of radiation and suction parameters reduces heat conduction in Ethylene glycol based nanofluid. The effect of ϕ on $\theta(\eta)$ is exhibited in Figure 6, while that of the porosity parameter on $\theta(\eta)$ is shown in Figure 7. Both parameters enhance the thermal transfer in nanofluid flow, but the opposite result is given by the radiation and suction parameters, as shown in Figures 8 and 9, respectively. Further, the presence of Fe_3O_4 nanoparticle enhances with the temperature profile. This is because Fe_3O_4 particles have high thermal conductivity, so the thermal boundary layer thickness increases. The porosity parameter also develops the thermal boundary layer thickness. However, the presence of thermal radiation and suction parameters are reduces the thermal boundary layer thickness.

The impacts of the heat sink or source parameter with respect to the heat profile are presented in Figure 10. It generates energy in the boundary layer, which is caused by the heat source ($\beta > 0$) on the heat profile. Energy is absorbed in the boundary layer, which arises from the heat sink ($\beta < 0$) on the heat profile.

5. 2. Nusselt Number and Skin Friction Figure 11 represent the effect of skin friction coefficient $-f''(0)$ for various values of Hartmann number and nanosolid volume fraction parameters against suction parameter. The skin friction coefficient $-f''(0)$ diminish for higher values of ϕ while the overturn trend is checked for large value of Hartmann number. Against Hartmann number, the different values of radiation, suction, nanosolid volume fraction parameters on Nusselt number has been

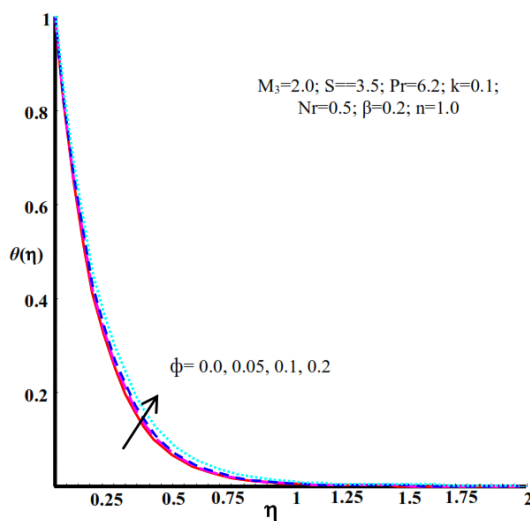


Figure 6. Impact of nanoparticles volume fraction parameter on $\theta(\eta)$

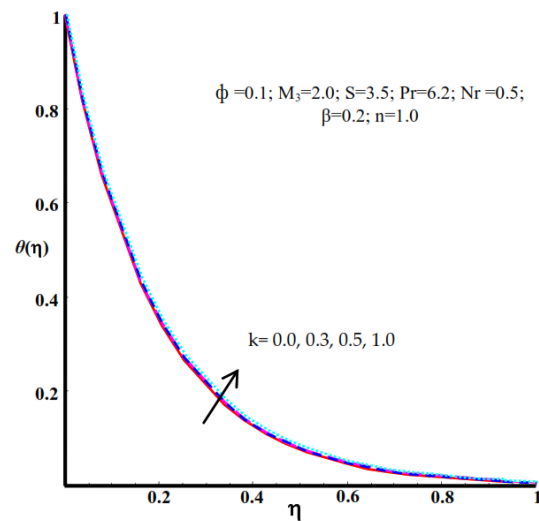


Figure 7. Impact of porosity parameter on $\theta(\eta)$

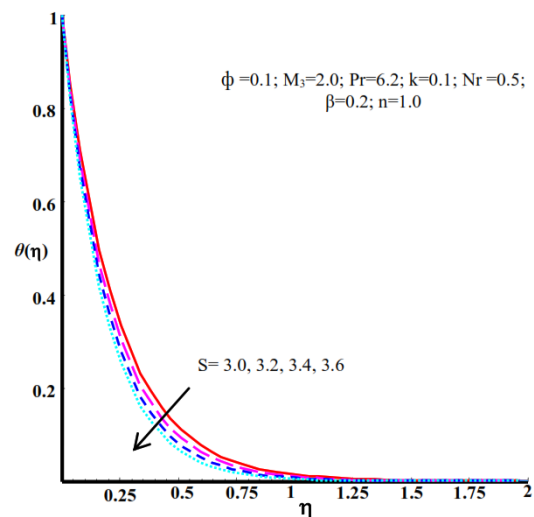


Figure 8. Impact of suction parameter on $\theta(\eta)$

depicted in Figure 12. The heat transfer rate improved with large value of radiation and suction parameters and reduced value of nanosolid volume fraction.

5. 3. Bejan Number and Entropy Generation

The effects of the porosity, heat sink or source, nanosolid volume fraction, radiation, suction parameters pertaining to the entropy generation profile are presented in Figures 13-17. In Fe_3O_4 -ethylene glycol nanofluid, the entropy generation increases with the increase in the suction and heat sink ($\beta < 0$) parameters. Furthermore, the presence of heat source ($\beta > 0$), radiation, porosity, nanosolid volume fraction parameters diminishes the production of entropy. The characteristics of entropy generation with respect to ϕ are shown in Figure 13. Figure 14 indicates the results of entropy generation for different porosity parameters. The effects of the suction parameter on N_s are shown in

Figure 15. Figures 16 and 17 depict the characteristics of radiation and heat sink or source parameters, respectively. It is clear that the presence of Fe_3O_4 nanofluid volume fraction, porosity parameter, thermal radiation, uniform heat source parameters are control the more entropy production. But the suction parameter develop the entropy production.

The influence of Bejan number with respect to various physical parameters like Brinkman number, nanosolid volume fraction, heat sink or source, suction parameters have been depicted in Figures 18-21. From the figures, the Bejan number is improved with the heat source ($\beta > 0$) and nanosolid volume fraction parameters, but is reduced with the heat sink ($\beta < 0$), suction and Brinkman number. Figure 18 shows the variation of ϕ on Be. Figure 19. depicts the impact of S on Be. Figures 20 and 21 indicate the results of Be with respect to different values of Brinkman number and heat sink or source parameters, respectively.

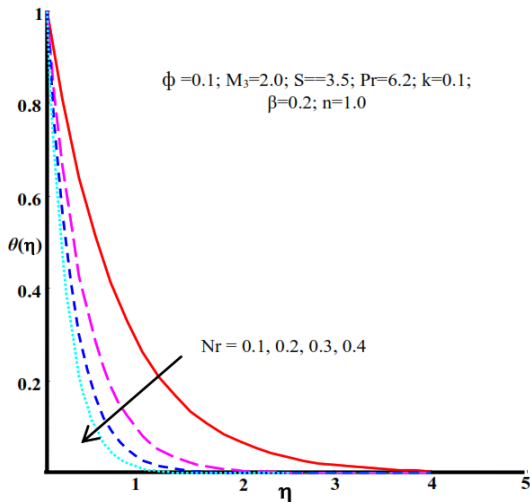


Figure 9. Impact of radiation parameter on $\theta(\eta)$

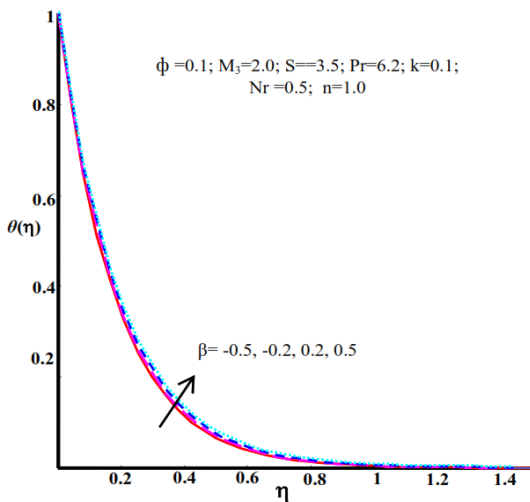


Figure 10. Impact of β on $\theta(\eta)$

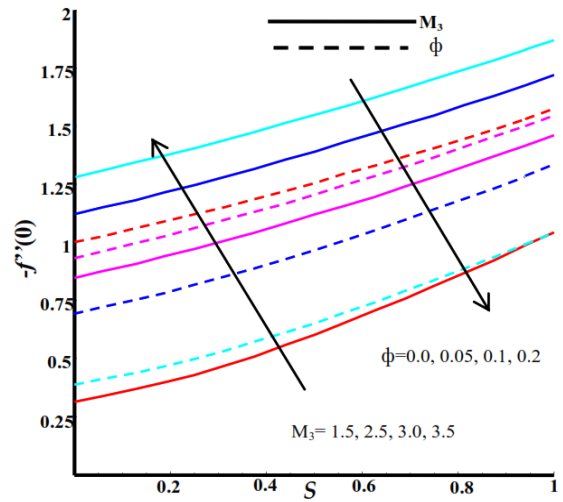


Figure 11. Impact of ϕ and M_3 on $-f'(0)$

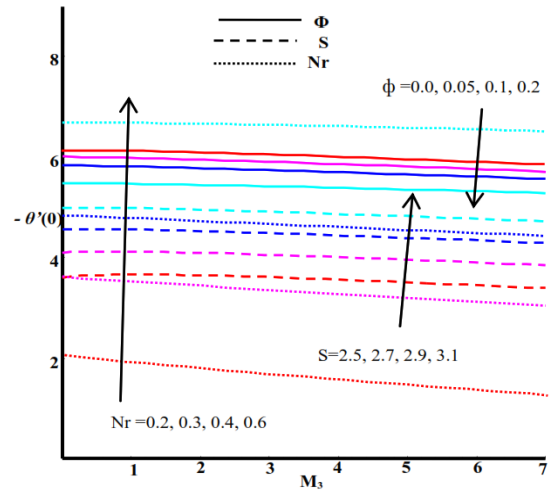


Figure 12. Impact of ϕ , S and Nr on $-\theta'(0)$

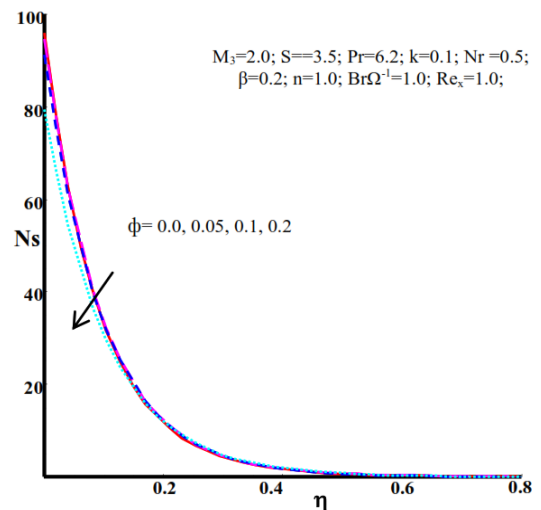


Figure 13. Impact of nanoparticles volume fraction parameter on N_s

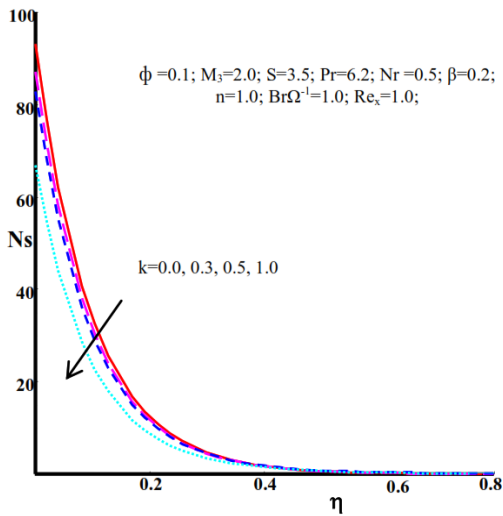


Figure 14. Impact of porosity parameter on Ns

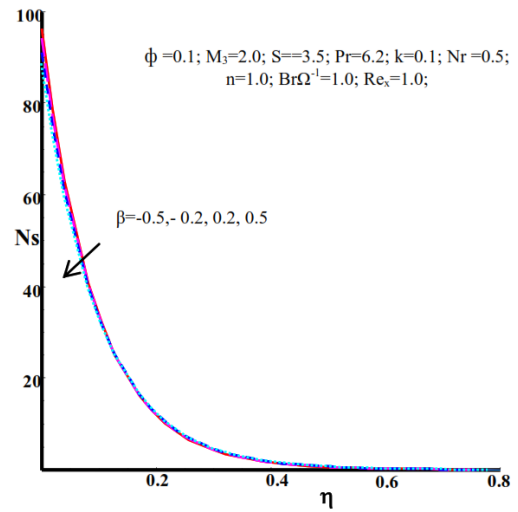


Figure 17. Impact of heat source/sink parameter on Ns

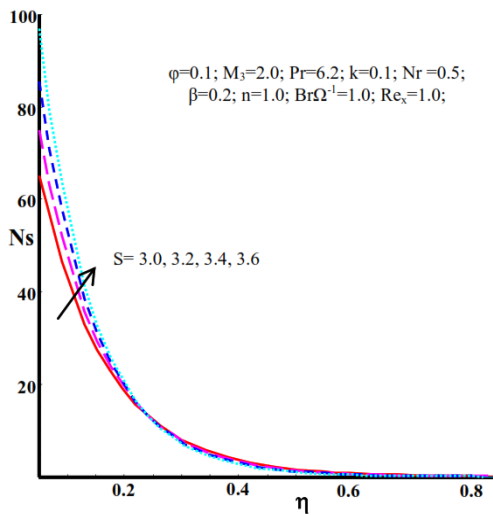


Figure 15. Impact of suction parameter on Ns

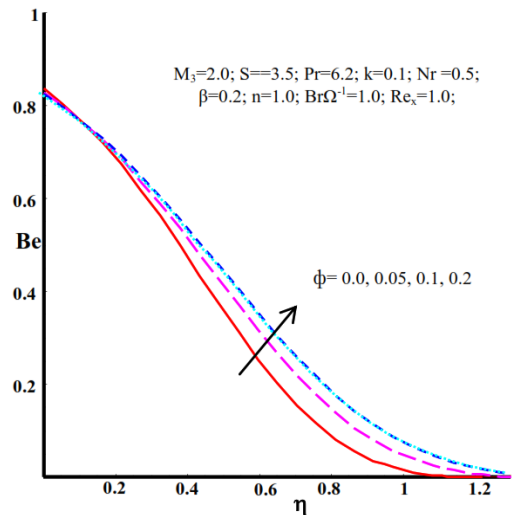


Figure 18. Impact of nanoparticles volume fraction parameter on Be

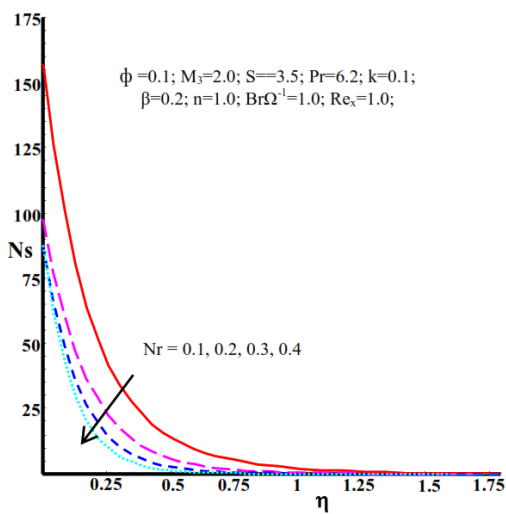


Figure 16. Impact of radiation parameter on Ns

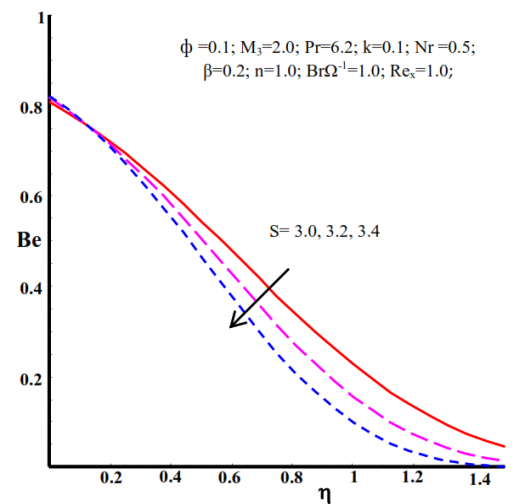


Figure 19. Impact of suction parameter on Be

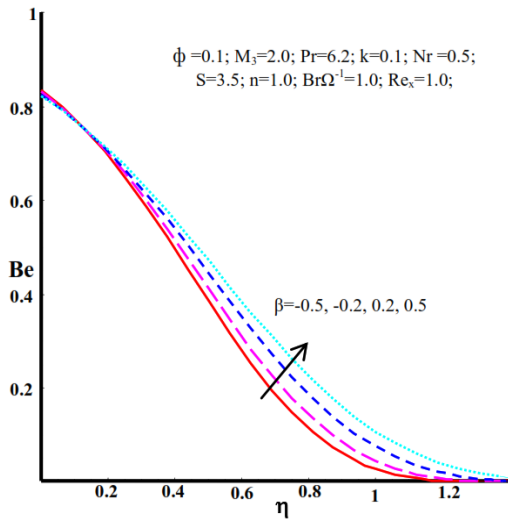


Figure 20. Effect of heat source/sink parameter on Be

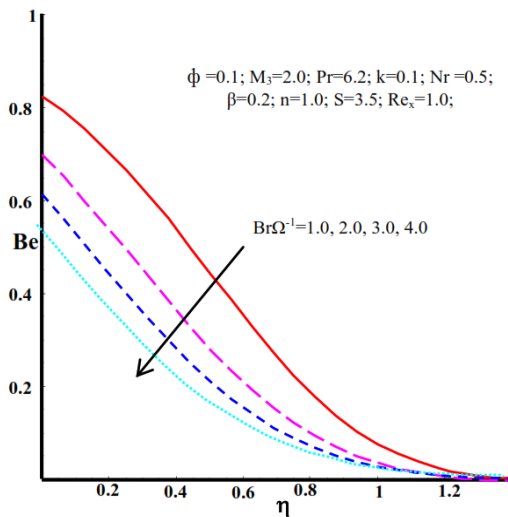


Figure 21. Impact of $Br\Omega^{-1}$ on Be

TABLE 1. Thermo-physical properties of ethylene glycol and nanoparticles [42]

	$\rho(\text{kg/m}^3)$	$C_p(\text{J/kgK})$	$k(\text{W/m.K})$
Ethylene glycol	1110	2400	0.26
Fe_3O_4	5200	670	6

TABLE 2. Evaluate solution of Skin friction for different values of S with $M_3 = 2$ When $\phi=k=0$

S	[39]	[40]	Present results
2	2.414214	2.414217	2.41421
3	3.302776	3.302772	3.30278
4	4.236068	4.236073	4.23607

6. CONCLUSIONS

We have presented an analytical approach pertaining to entropy generation on Fe_3O_4 -Ethylene glycol MHD nanofluid through a shrinking wall with porous medium in the presents of heat sink or source and thermal radiation. We have obtained the important results, as follows:

- The velocity of Fe_3O_4 -ethylene glycol nanofluid is enhanced with the increase in the suction parameters, but it slows down with respect to the nanosolid volume fraction and porosity parameters. The heat of Fe_3O_4 -Ethylene glycol nanofluid is enhanced with the increase in the heat source, nanosolid volume fraction and porosity and it decreases with the heat sink, suction and radiation parameters. The presence of Fe_3O_4 nanoparticle enhances with the temperature profile. This is because Fe_3O_4 particles have high thermal conductivity, so the thermal boundary layer thickness increases. The porosity parameter also develops the thermal boundary layer thickness. But the presence of thermal radiation and suction parameters reduces the thermal boundary layer thickness.
- The skin friction increases with the Hartmann number, but decreases with nanosolid volume fraction. The Nusselt number is enhanced with radiation and suction parameters, but it is reduced with nanosolid volume fraction.
- The entropy generation profile is maximized with suction and heat sink, but it is minimized with nanosolid volume fraction, porosity and heat source. It is clear that the presence of Fe_3O_4 nanofluid volume fraction, porosity parameter, thermal radiation, uniform heat source parameters are control the more entropy production. But the suction parameter develops the entropy production.

The Bejan number increases with nanosolid volume fraction and heat source, but decreases with suction, Brinkman number and heat sink. In the future, this paper can be extended for different nanofluids considering the effect of magnetic field with nonlinear thermal radiation in different types of boundary conditions.

7. REFERENCES

1. Choi, S.U.S., "Enhancing thermal conductivity of fluids with nanoparticles", In: Proceedings of the 1995 ASME International Mechanical Engineering Congress and Exposition, San Francisco, Calif, USA, Vol. 66, (1995), 99-105
2. Ibrahim, W., Shankar, B., Nandeppanavar, M. M., "MHD stagnation point flow and heat transfer due to nanofluid towards a stretching sheet", *International Journal of Heat and Mass Transfer*, Vol. 56, (2013) 1-9. DOI: 10.1016/j.ijheatmasstransfer.2012.08.034

3. Hayat, T., Imtiaz, M., Alsaedi, A., Mansoor, R., "MHD flow of nanofluids over an exponentially stretching sheet in a porous medium with convective boundary conditions", *Chinese Physics B*, Vol. 23, No. 5, (2014), 054701. DOI:10.1088/1674-1056/23/5/054701
4. Malvandi A., Ganji D. D., "Magnetohydrodynamic mixed convective flow of Al₂O₃-water nanofluid inside a vertical micro tube", *Journal of Magnetism and Magnetic Materials*, Vol. 369, (2014), 132-141. DOI: 10.1016/j.jmmm.2014.06.037
5. Rahman, M. M., Rosca, A. V., Pop, I., "Boundary layer flow of a nanofluid past a permeable exponentially shrinking/stretching surface with second order slip using Buongiorno's model", *International Journal of Heat and Mass Transfer*, Vol. 77, (2014), 1133-1143. DOI: 10.1016/j.ijheatmasstransfer.2014.06.013
6. Shaha, Z., Ebraheem, O., Alzahrani, B., Abdullah, D., Asad, U., Ikrumullah K., "Influence of Cattaneo-Christov model on Darcy-Forchheimer flow of Micropolar Ferrofluid over a stretching/shrinking sheet", *International Communications in Heat and Mass Transfer*, Vol. 110, (2020), 104385. DOI: 10.1016/j.icheatmasstransfer.2019.104385
7. Sheikholeslami, M., Bandpy, M. G., Ellahi, R., Zeeshan A., "Simulation of MHD CuO-water nanofluid flow and convective heat transfer considering Lorentz forces", *Journal of Magnetism and Magnetic Materials*, Vol. 369, (2014) 69-80. DOI: 10.1016/j.jmmm.2014.06.017
8. Jamaludin, A., Naganthran, K., Nazar, R., Pop, I., "MHD mixed convection stagnation-point flow of Cu-Al₂O₃/water hybrid nanofluid over a permeable stretching/shrinking surface with heat source/sink", *European Journal of Mechanics / B Fluids*, Vol. 84, (2020), 71-80. DOI: 10.1016/j.euromechflu.2020.05.017
9. Dero, S., Rohni, A. M., Saaban, A., "Stability analysis of Cu-C₆H₉NaO₇ and Ag-C₆H₉NaO₇ nanofluids with effect of viscous dissipation over stretching and shrinking surfaces using a single phase model", *Heliyon*, Vol. 6, (2020), 03510. DOI: 10.1016/j.heliyon.2020.e03510
10. Haq, R. U., Raza, A., Ebrahem A., Algehyne, Tili, I., "Dual nature study of convective heat transfer of nanofluid flow over a shrinking surface in a porous medium", *International Communications in Heat and Mass Transfer*, Vol. 114, (2020), 104583. DOI: 10.1016/j.icheatmasstransfer.2020.104583
11. Shah Naqvi, S.M.R., Muhammad, T., Saleem, S., Kim, H.M., "Significance of non-uniform heat generation/absorption in hydromagnetic flow of nanofluid due to stretching/shrinking disk", *Physica A*, Vol. 553, (2020), 123970. DOI: 10.1016/j.physa.2019.123970
12. Khan, U., Zaib, A., Zahir S., Dumitru B., El-Sayed M. Sherif, "Impact of magnetic field on boundary-layer flow of Sisko liquid comprising nanomaterials migration through radially shrinking/stretching surface with zero mass flux", *Journal of Material Research and Technology*, Vol. 9, No. 3, (2020), 3699-3709. DOI: 10.1016/j.jmrt.2020.01.107
13. Khashi'ie, N. S., Arifina, N. M., Pop, I., Nazar, R., Hafidzuddin, E.H., Wahi, N., "Three-Dimensional Hybrid Nanofluid Flow and Heat Transfer past a Permeable Stretching/Shrinking Sheet with Velocity Slip and Convective Condition", *Chinese Journal of Physics*, Vol. 66, (2020), 157-171. DOI: 10.1016/j.cjph.2020.03.032
14. Gireesha, B. J., Umeshaiyah, M., Prasannakumara, B. C., Shashikumar N. S., Archana, M., "Magnetohydrodynamic three dimensional boundary layer flow of Jeffrey nanofluid over a nonlinearly permeable stretching sheet", *Physica A*, Vol. 549, (2020), 124051. DOI: 10.1016/j.physa.2019.124051
15. Hayat, T., Kanwal, M., Qayyum, S., Alsaedi, A., "Entropy generation optimization of MHD Jeffrey nanofluid past a stretchable sheet with activation energy and non-linear thermal radiation", *Physica A: Statistical Mechanics and its Applications*, Vol. 544, (2020), 123437. DOI: 10.1016/j.physa.2019.123437
16. Hosseinzadeh, K. H., Mogharebi, A. R., Asadi, A., Sheikhshahrokhdehordi, M., Seyedmohammad M., Ganji, D.D., "Entropy generation analysis of mixture nanofluid (H₂O/C₂H₆O₂)-Fe₃O₄ flow between two stretching rotating disks under the effect of MHD and nonlinear thermal radiation", *International Journal of Ambient Energy*, (2019), 1-13. DOI: 10.1080/01430750.2019.1681294
17. Shahsavari, A., Moradi, M., Bahiraie, M., "Heat transfer and entropy generation optimization for flow of a non-Newtonian hybrid nanofluid containing coated CNT/Fe₃O₄ nanoparticles in a concentric annulus", *Journal of the Taiwan Institute of Chemical Engineers*, (2018), 1-13. DOI: 10.1016/j.jtice.2017.12.029
18. Mehrali, M., Sadeghinezhad, E., Akhiani, A.R., Latibari, S.T., Metselaar, H.S.C., Kherbeet, A.S., Mehrali, M., "Heat transfer and entropy generation analysis of hybrid graphene/Fe₃O₄ ferro-nanofluid flow under the influence of a magnetic field", *Powder Technology*, Vol. 308, (2017), 149-157. DOI: 10.1016/j.powtec.2016.12.024
19. López, A., Ibáñez, G., Pantoja, J., Moreira, J., Lastres, O., "Entropy generation analysis of MHD nanofluid flow in a porous vertical microchannel with nonlinear thermal radiation, slip flow and convective-radiative boundary conditions", *International Journal of Heat and Mass Transfer*, Vol. 107, (2017), 982-994. DOI: 10.1016/j.ijheatmasstransfer.2016.10.126
20. Shukla, N., Rana, P., Anwar Bégb, O., Bani S., Kadir, A., "Homotopy study of magnetohydrodynamic mixed convection nanofluid multiple slip flow and heat transfer from a vertical cylinder with entropy generation", *Propulsion and Power Research*, Vol. 8, (2019), 147-162. DOI: 10.1016/j.jprr.2019.01.005
21. Hayat, T., Rabiya Y., Sumaira Q., Alsaedi, A., "Entropy generation optimization in nanofluid flow by variable thicked sheet", *Physica A: Statistical Mechanics and its Applications*, Vol. 551, (2020). DOI: https://doi.org/10.1016/j.physa.2019.124022
22. Rana, P., Shukla, N., "Entropy generation analysis for non-similar analytical study of nanofluid flow and heat transfer under the influence of aligned magnetic field", *Alexandria Engineering Journal*, Vol. 57, (2018), 3299-3310. DOI: https://doi.org/10.1016/j.aej.2017.12.007
23. Govindaraju, M., Ganga, B., Abdul Hakeem, A.K., "Second law analysis on radiative slip flow of nanofluid over a stretching sheet in the presence of Lorentz force and heat generation/absorption", *Frontiers in Heat and Mass Transfer (FHMT)*, Vol. 8, No. 10, (2017), 1-10. DOI: http://dx.doi.org/10.5098/hmt.8.10
24. Abdul Hakeem, A. K., Govindaraju, M., Ganga, B., Kayalvizhi, M., "Second law analysis for radiative MHD slip flow of a nanofluid over a stretching sheet with non-uniform heat source effect", *ScientiaIranica F*, Vol. 23, No. 3, (2016), 1524-1538. DOI: 10.24200/SCI.2016.3916
25. Ganga, B., Govindaraju, M., Abdul Hakeem, A.K., "Effects of Inclined Magnetic Field on Entropy Generation in Nanofluid Over a Stretching Sheet with Partial Slip and Nonlinear Thermal Radiation", *Iranian Journal of Science and Technology, Transactions of Mechanical Engineering*, (2018), 1-12. DOI: https://doi.org/10.1007/s40997-018-0227-0
26. Rashid, S., Sagheer, M., Hussain, S., "Entropy formation analysis of MHD boundary layer flow of nanofluid over a porous shrinking wall", *Physica A*, Vol. 536, (2019), 122608. https://doi.org/10.1016/j.physa.2019.122608

27. Seth, G. S., Bhattacharyya, A., Kumar, R., Chamkha, A. J., "Entropy generation in hydromagnetic nanofluid flow over a non-linear stretching sheet with Navier's velocity slip and convective heat transfer", *Physics of Fluids*, Vol. 30, (2018), 122003. DOI: <https://doi.org/10.1063/1.5054099>
28. Acharya, N., Das, K., Kumar Kundu, P., "On the heat transport mechanism and entropy generation in a nozzle of liquid rocket engine using ferrofluid: A computational framework", *Journal of Computational Design and Engineering*, Vol. 6, (2019), 739-750. DOI: <https://doi.org/10.1016/j.jcde.2019.02.003>
29. Daniel, Y. S., Abdul Aziz, Z., Ismail, Z., Salah, F., "Entropy analysis in electrical magnetohydrodynamic (MHD) flow of nanofluid with effects of thermal radiation, viscous dissipation, and Chemical reaction", *Theoretical & Applied Mechanics Letters*, Vol. 7, (2017), 235-242. DOI: <https://doi.org/10.1016/j.taml.2017.06.003>
30. Ellahi, R., Sultan Z A., Abdul B., Majeed, A., "Effects of MHD and slip on heat transfer boundary layer flow over a moving plate based on specific entropy generation", *Journal of Taibah University for Science*, Vol. 12, No. 4, (2018), 476-482. DOI: <https://doi.org/10.1080/16583655.2018.1483795>
31. Sheikholeslami M., "New computational approach for exergy and entropy analysis of nanofluid under the impact of Lorentz force through a porous media", *Computer Methods in Applied Mechanics and Engineering*, Vol. 344, (2019), 319-33. DOI: <https://doi.org/10.1016/j.cma.2018.09.044>
32. Riaz, A., Bhatti, M.M., Ellahi, R., Zeeshan, A., Sait, S.M., "Mathematical analysis on an asymmetrical wavy motion of blood under the influence entropy generation with convective boundary conditions", *Symmetry*, Vol. 2, No. 1, (2020), 102. DOI: <https://doi.org/10.3390/sym12010102>
33. Döner, A., Comparison of corrosion behaviors of bare Ti and TiO₂, *Emerging Science Journal*, Vol. 3, No. 4, (2019), 235-240. DOI: <http://dx.doi.org/10.28991/esj-2019-01185>
34. Slavova, M., Mihaylova Dimitrova, E., Mladenova, E., Abrashev, B., Burdin, B., Vladikova, D., "Zeolite based air electrodes for secondary batteries", *Emerging Science Journal*, Vol. 4, No. 1, (2020), 18-24. DOI: <http://dx.doi.org/10.28991/esj-2020-01206>
35. Kostikov, Y. A., Romanenkov, A. M., "Approximation of the multidimensional optimal control problem for the heat equation (Applicable to computational fluid dynamics (CFD))", *Civil Engineering Journal*, Vol. 6, No. 4, (2020), 743-768. DOI: [10.28991/cej-2020-03091506](https://doi.org/10.28991/cej-2020-03091506)
36. Kostikov, Y. A., Romanenkov, A. M., "The technology of calculating the optimal modes of the disk heating (Ball)", *Civil Engineering Journal*, Vol. 5, No. 6, (2019), 1395-1406. DOI: [10.28991/cej-2019-03091340](https://doi.org/10.28991/cej-2019-03091340)
37. Theingi, M., ThiTun, K., Aung, N. N., "Preparation, characterization and optical property of LaFeO₃ nanoparticles via Sol-Gel combustion method", *SciMedicine Journal*, Vol. 1, No. 3, (2019), 151-157.
38. Zhang, W., Yang, X., Wang, T., Peng, X., Wang, X., "Experimental study of a gas engine driven heat pump system for space heating and cooling", *Civil Engineering Journal*, Vol. 5, No. 10, (2019), 2282-2295. DOI: [10.28991/cej-2019-03091411](https://doi.org/10.28991/cej-2019-03091411)
39. Muhaimin., Kandasamy, R., Azme B. Khamis., "Effects of heat and mass transfer on nonlinear MHD boundary layer flow over a shrinking sheet in the presence of suction", *Applied Mathematics and Mechanics*, Vol. 29, No. 10, (2008), 1309-1317. DOI: [10.1007/s10483-008-1006-z](https://doi.org/10.1007/s10483-008-1006-z)
40. Bhattacharyya, K., "Effects of radiation and heat source/sink on unsteady MHD boundary layer flow and heat transfer over a shrinking sheet with suction/injection", *Frontiers of Chemical Science and Engineering*, Vol. 5, No. 3, (2011), 376-384. DOI: [10.1007/s11705-011-1121-0](https://doi.org/10.1007/s11705-011-1121-0)
41. Rashid, I., Rizwan UlHaq., Khan, Z. H., Qasem M. Al-Mdallal., "Flow of water based Alumina and Copper nanoparticles along a moving surface with variable temperature", *Journal of Molecular Liquids*, Vol. 246, (2017), 354-362. DOI: [10.1016/j.molliq.2017.09.089](https://doi.org/10.1016/j.molliq.2017.09.089)
42. Sheikholeslami, M., Shamlooei, M., Moradi, R., "Fe₃O₄-Ethylene glycol nanofluid forced convection inside a porous enclosure in existence of Coulomb force", *Journal of Molecular Liquids*, Vol. 249, (2018), 427-439. DOI: [10.1016/j.molliq.2017.11.048](https://doi.org/10.1016/j.molliq.2017.11.048)

Persian Abstract

چکیده

این تحقیق عمدتاً بر تأثیرات جذب / تولید گرما و تابش بر جریان هیدرو مغناطیسی نانوسیال Fe₃O₄-اتیلن گلیکول از طریق دیواره کوچک شده با محیط متخلخل و محاسبه تولید آنتروپی متمرکز است. ما معادلات دیفرانسیل معمولی حاکم را با استفاده از راه‌حل‌های مشابه مناسب به معادلات دیفرانسیل جزئی در نظر می‌گیریم. علاوه بر این، عملکرد هندسی بیش از حد برای تعیین مسئله فرموله شده استفاده می‌شود. ما اثرات پارامترهای فیزیکی مناسب را بر روی تعداد Bejan، تولید آنتروپی، تعداد Nussult، اصطکاک پوست، دمای مایع و پروفیل سرعت تجزیه و تحلیل می‌کنیم. علاوه بر این، نتیجه حاصل از مطالعه حاضر با نتایج موجود در ادبیات موجود مقایسه می‌شود. ما متذکر شدیم که وجود پارامترهای جذب حرارت و مکش، تعداد Bejan را کاهش می‌دهد و باعث افزایش تولید آنتروپی می‌شود و پارامترهای تابش منبع حرارت، محیط متخلخل، تولید آنتروپی را به حداقل می‌رساند. وجود پارامتر تخلخل سرعت سیال را کاهش می‌دهد، دمای سیال را بهبود می‌بخشد و تولید آنتروپی را به حداقل می‌رساند. پارامتر کسری حجمی نانوسیال هم تعداد Nussult و هم ضریب اصطکاک پوست را کاهش داد.
